Project information	
Project full title	EuroSea: Improving and Integrating European Ocean Observing and Forecasting Systems for Sustainable use of the Oceans
Project acronym	EuroSea
Grant agreement number	862626
Project start date and duration	1 November 2019, 50 months
Project website	https://www.eurosea.eu

Deliverable information	
Deliverable number	D4.10
Deliverable title	**Results of the BGC data assimilation**
Description	
Work Package number	4
Work Package title	Data integration, Assimilation, and Forecasting
Lead beneficiary	OGS
Lead authors	Gianpiero Cossarini
Contributors	Carolina Amadio, Anna Teruzzi, Ali Aydogdu, Jenny Pistoia, Jaime Hernandez, Baptiste Mourre
Due date	30 April 2023
Submission date	28 April 2023
Comments	

This project has received funding from the European Union's Horizon 2020 research and innovation programme under grant agreement No. 862626.

https://doi.org/10.3289/eurosea_d4.10

Table of contents

Executive summary

This document presents the results of simulations that include glider profiles assimilation. Simulations are performed with the Marine Copernicus operational biogeochemical model system of the Mediterranean Sea. The deliverable shows that the assimilation of BGC-glider is feasible in the contest of biogeochemical operational systems and that it is built upon the experience of BGC-Argo float data assimilation. Different configuration of the assimilation of glider data have been tested to assess the impact of the physical and biogeochemical glider observations. The deliverable also describes the pre-processing activities of the BGC-glider data to provide qualified observations for the data assimilation and the cross validation of chlorophyll glider data with other sensors (ocean colour and BGC-Argo floats).

Results of the simulations show that BGC-glider data assimilation, as already shown for BGC-Argo floats, provides complementary information with respect to Ocean Colour data (which is the only or the most commonly assimilated data in biogeochemical operational systems). Beside their relatively limited horizontal spatial impact, the assimilation of BGC profiles can constrain model simulations for relevant biogeochemical processes in specific periods (summer and transition periods) and layers (surface and subsurface). Results also highlight the importance of the assimilation modelling systems that can efficiently resolve the inconsistencies between chlorophyll observations of different sensors.

1. Introduction

The objectives of the present deliverable are to evaluate the impact of physical glider assimilation on biogeochemistry and the assessment of the feasibility and benefit of biogeochemical profile (BGC-Argo float and BGC-glider) assimilation on the analysis and forecast quality of the MedBFM model system. The MedBFM is the biogeochemical modelling system that provides analysis, short term forecast (Salon et al., 2019) and long-term reanalysis (Cossarini et al., 2021) of the Mediterranean Sea for the Copernicus Marine Service.

Within the framework of operational oceanography (such as the Marine Copernicus Service) the biogeochemical assimilation mainly relies on satellite ocean colour observation (Fennel et al., 2019). Chlorophyll concentration is the most commonly assimilated ocean colour variable (Nerger and Gregg, 2007, 2008; Hu et al., 2012; Fontana et al., 2013; Gehlen et al., 2015; Ciavatta et al., 2016; Ford and Barciela, 2017; Tsiaras et al., 2017; Mattern et al., 2018; Teruzzi et al., 2018; Pradhan et al., 2019), given its unique capability to provide frequent, high coverage and high resolution (up to 1 km in Marine Copernicus Service) observations of the biological components of the surface of the ocean. However, the propagation of surface information towards deeper marine layers requires approximations such as parameterization of vertical covariances (Teruzzi et al., 2018) or inclusion of localization terms in ensemble filters and can have limitation in deeper ocean layer (Hu et al., 2012; Fontana et al., 2013; Simon et al., 2015). On the other hand, in situ profile observations bring information on processes occurring in the ocean interior (e.g., deep chlorophyll maximum, vertical fluxes of nutrients and organic matter). Operational autonomous sensors, such as BGC-Argo floats or BGC-gliders, provide frequent and high-resolution water column descriptions for open sea and coastal areas (Bittig et al., 2019; Testor et al., 2019). Despite their importance, there are only few examples of assimilation of in situ biogeochemical profiles. Cossarini et al. (2019), Teruzzi et al. (2021) and Verdy and Mazloff (2017) assimilated BGC-Argo floats improving vertical variability of biogeochemical processes (e.g.,

the depth of the deep chlorophyll maximum). Kaufman et al. (2018) showed that the assimilation of BGC data from gliders is effective to constrain depth-integrated primary production and carbon export.

The present work is built upon (i) the publication by Teruzzi et al. (2021) that shows the impact of the BGC-Argo float data assimilation in the Mediterranean biogeochemical model system and (ii) the novel developments for the assimilation of BGC-glider data.

The present deliverable is subdivided as follows: section 2 briefly describes the biogeochemical Mediterranean model system of the Marine Copernicus Service with a focus on the developments of vertical profile data assimilation (section 2.3). The novel work done for the development of BGC-glider assimilation are described in sections 3 and 4. Results showing the impact of physical-glider and BGC-glider assimilation on biogeochemistry are presented in section 5. Conclusions are drawn in section 6.

2. The Mediterranean biogeochemical model system

MedBFM system consists of the coupled physical-biogeochemical OGSTM-BFM model and the 3DVarBio assimilation scheme (Figure 1; Lazzari et al., 2010, 2012, 2016; Teruzzi et al., 2014, 2018, 2019; Cossarini et al., 2015; Cossarini et al., 2019; Salon et al., 2019). It is the official model system for the biogeochemical component of the Mediterranean Sea of the Marine Copernicus Service (Salon et al., 2019; Coppini et al., 2023).

2.1. OGSTM-BFM model

OGSTM model is a modified version of the OPA 8.1 transport model (Foujols et al., 2000), which resolves the advection, the vertical diffusion and the sinking terms of the tracers (biogeochemical variables). The OGSTM resolves the free surface and variable volume layer effects on the transport of tracers being fully consistent with NEMO3.6 vvl output provided by Med-PHY. The horizontal meshgrid is based on 1/24° longitudinal scale factor and on 1/24°cos(ϕ) latitudinal scale factor. The vertical discretization accounts for 141 vertical z-levels, with 125 actives in the Mediterranean domain: 35 in the first 200 m depth, 60 between 200 and 2000 m, 30 below 2000 m. The temporal scheme of OGSTM is an explicit forward time scheme for the advection and horizontal diffusion terms, whereas an implicit time step is adopted for the vertical diffusion.

The sinking term is a vertical flux, which acts on a sub-set of the biogeochemical variables (particulate matter and phytoplankton groups). Sinking velocity is fixed for particulate matter and dependent on nutrients for two phytoplankton groups (diatoms and dinoflagellates).

The daily mean hydrodynamical forcing is provided by the Mediterranean physical model system (Clementi et al., 2022), which supplies the temporal evolution of the fields of horizontal and vertical current velocities, vertical eddy diffusivity, potential temperature, salinity, sea surface height in addition to surface fields for solar shortwave irradiance and wind stress (see section on upstream data and boundary conditions for further details)

The features of the biogeochemical reactor BFM (Biogeochemical Flux Model) have been chosen to target the energy and material fluxes through both “classical food chain” and “microbial food web” pathways (Thingstad and Rassoulzadegan, 1995), and to consider co-occurring effects of multi-nutrient interactions. Both factors are particularly important in the Mediterranean Sea, wherein microbial activity fuels the trophodynamics of a large part of the system for much of the year and both phosphorus and nitrogen can

play limiting roles (Krom et al., 1991; Bethoux et al., 1998). BFM has been upgraded including the use of multispectral light for photosynthesis and interaction between light and biogeochemistry (Lazzari et al., 2021). BFMv5 model (i.e., the official version released by www.bfm-community.eu) describes the biogeochemical cycles of 4 chemical compounds: carbon, nitrogen, phosphorus and silicon through the dissolved inorganic, living organic and non-living organic compartments. The model includes nine plankton functional types (PFTs). Phytoplankton PFTs are diatoms, flagellates, picophytoplankton and dinoflagellates. Heterotrophic PFTs consist of carnivorous and omnivorous mesozooplankton, bacteria, heterotrophic nanoflagellates and microzooplankton. Nitrate and ammonia are considered for the dissolved inorganic nitrogen. The non-living compartment consists of 3 groups: labile, semilabile and refractory organic matter. The first two are described in terms of carbon, nitrogen, phosphorus and silicon contents. The model is fully described in Lazzari et al. (2012, 2016), where it was corroborated for chlorophyll, primary production and nutrients in the Mediterranean Sea for a 1998-2004 simulation. The BFM model is also coupled to a carbonate system model (Cossarini et al., 2015, Canu et al., 2015), which consists of three prognostic state variables: alkalinity (ALK) and dissolved inorganic carbon (DIC) and particulate inorganic carbon (PIC). pCO2 and pH (expressed in total scale) are calculated at the in-situ temperature and pressure conditions using Mehrbach et al. (1973) refit by Lueker et al. (2000). Formulations for the kinetic constants of thermodynamic equilibrium of carbon acid dissociation as prescribed in Orr and Epitaloni (2015). CO2 air-sea gas exchange formulation is computed according to updates provided by Wanninkhof (2014).

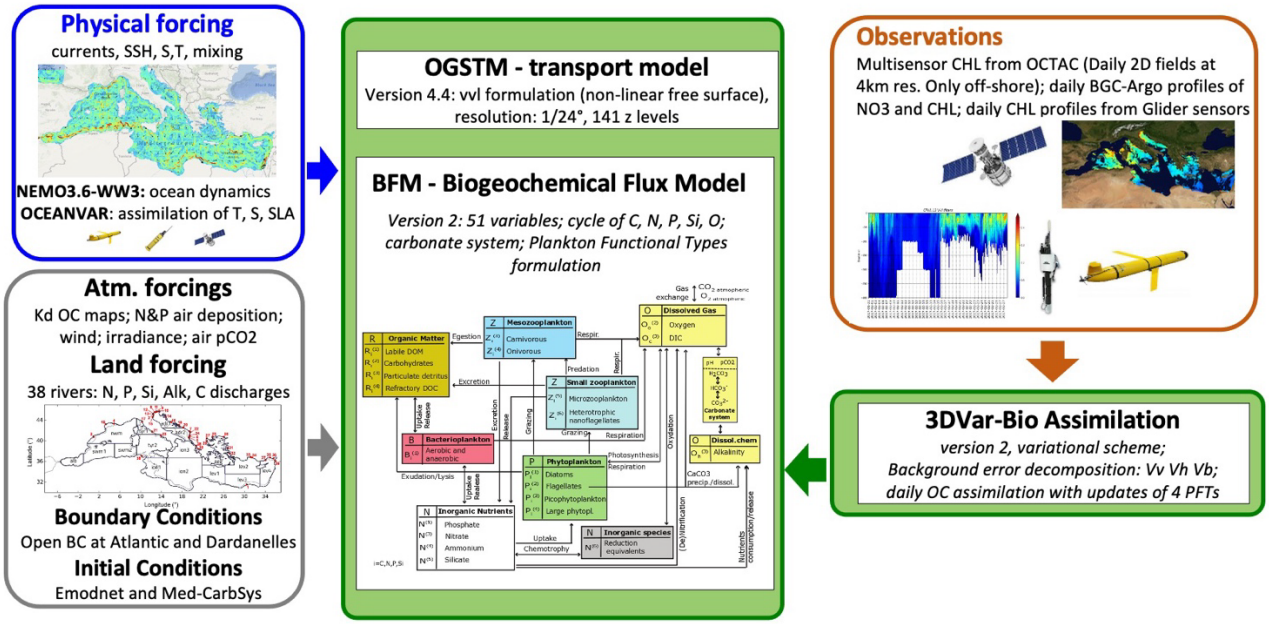

Figure 1. Scheme of the MedBFM model system (green boxes) and input data (ocean dynamics, blue box; setup, grey box) and assimilated observations (orange box)

2.2. 3DVar-Bio data assimilation scheme

In the variational 3DVarBio scheme (Teruzzi et al., 2014), the assimilation is performed through the minimization of a cost function:

$$J(\boldsymbol{x}_a) = (\boldsymbol{x}_a - \boldsymbol{x}_b)^T \mathbf{B}^{-1} (\boldsymbol{x}_a - \boldsymbol{x}_b) + (\boldsymbol{y} - H(\boldsymbol{x}_b))^T \mathbf{R}^{-1} (\boldsymbol{y} - H(\boldsymbol{x}_b))$$

where the increments (x_a -x_b) are weighted by the background error covariance matrix B and the misfits (y - H(x_b)) are weighted by the observation error matrix. The observation operator (H) maps the values of model background state x_b in the observation space. The background error covariance matrix, B, is factorised as $B = VV$, where V is a sequence of linear operators: $V = V_B V_H V_V$. The operators describe different aspects of the error covariances: the vertical covariance (V_V), the horizontal covariance (V_H) and the covariance among biogeochemical variables (V_B). V_V is defined by a set of synthetic profiles that are evaluated by means of an Empirical Orthogonal Function (EOF) decomposition applied to a validated multi-annual 1998-2015 run (Teruzzi et al., 2018). EOFs are computed for 12 months and 30 coastal and open sea sub-regions in order to account for the variability of biogeochemical anomaly fields. V_H is built using a Gaussian filter whose correlation radius modulates the smoothing intensity. A non-uniform and direction-dependent correlation radius has been implemented (Teruzzi et al., 2018, Cossarini et al., 2019). V_B operator consists of monthly and sub-region varying covariances among the biogeochemical variables. Further, specifically for the assimilation of chlorophyll, the V_B operator includes a balance scheme that maintains the ratio among the phytoplankton groups and preserves the physiological status of the phytoplankton cells (i.e., preserve optimal values for the internal chlorophyll and carbon nutrients quota).

2.3. 3DVarBio upgrade for profile (BGC-Argo float) data assimilation

The 3DVarBio scheme was first developed for the assimilation of ocean colour chlorophyll (Teruzzi et al., 2014) as a component of the Mediterranean Analysis&Forecast model system of the Marine Copernicus Service. The scheme was upgraded with vertical assimilation capability in the frame of the Copernicus marine Service Evolution 2016-2018 project MASSIMILI (https://marine.copernicus.eu/it/about/research-development-projects/2016-2018/massimili), when the assimilation of BGC-Argo profiles of chlorophyll was developed and tested (Cossarini et al., 2019). The assimilation of BGC-Argo profiles of chlorophyll and nitrate was then implemented in the operational Mediterranean Analysis&Forecast model system (Teruzzi et al., 2021).

Several upgrades of the 3DVarBio scheme were necessary for the developments of the assimilation of vertical in situ profiles. The observation operator (H) was upgraded to interpolate model vertical spacing to the vertical observation discretization. A pre-operational smoothing of vertical observations was also included to filter out high frequency noise. The horizontal covariance operator V_H was upgraded to include an anisotropic (Teruzzi et al., 2018) and a non-uniform along depth (Cossarini et al., 2019; Teruzzi et al., 2021) component. In particular, the correlation length radius can vary both horizontally and along the vertical dimension to account for local scale of variability of the error covariances. A localization term for the vertical covariance operator (V_V) was introduced together with a recalculation of the EOFs term for chlorophyll and nitrate based on the new reanalysis of the Mediterranean Sea (Cossarini et al, 2021). Additionally, the biogeochemical operator (V_B) was updated. Now, the new assimilation scheme corrects the four phytoplankton functional groups (17 state variables including carbon, chlorophyll, nitrogen phosphorus and silicon internal quotas) and two nutrients (i.e., phosphate and nitrate). Finally, a specific tuning of the diagonal component the

observation error matrix for the vertical profile observation was developed (Cossarini et al., 2019; Teruzzi et al., 2021) to optimize the impact of BGC-Argo profile versus the Ocean Colour assimilation.

Results of the joint profiles (BGC-Argo float) and Ocean Colour assimilation (Teruzzi et al., 2021) revealed the assimilation of all the data streams outperformed the single-source assimilation when validated with respect to available observations, indicating that the assimilation of BGC-Argo observations has relevant impacts on the vertical structure of nutrients and phytoplankton. The impacts of multi-variate profile assimilation are directly linked to the sampling frequency and dimension of the BGC-Argo network, which should increase to match the consolidated importance and relevance of satellite observation assimilation. Interesting, the assimilation of vertical profiles improved the model capability to describe the dynamics and variability of the Deep Chlorophyll Maximum and nitracline in different areas of the Mediterranean Sea (Teruzzi et al., 2021).

The development of BGC-glider assimilation has been built upon the experience of the BGC-Argo float data assimilation. New specific developments have focused mainly on the preparation (pre-processing) of the BGC-glider observations (section 3) to be ready for assimilation. Section 4 summarizes the specificity of the setup of the 3DVarBio scheme for the BGC-glider assimilation.

3. Pre-processing for BGC-glider data

3.1. BGC-glider data

Availability and selection of the BGC-glider data is described in deliverable D4.2 and briefly summarized here. In order to balance data availability, data quality and data format, it was decided to focus the analysis on year 2017 and to use, as source of the glider observations, the product "INSITU_MED_NRT_OBSERVATIONS_013_035[1]" from the Copernicus Marine Service IN-SITU TAC website. Data were downloaded in November 2022 and, as described in the Copernicus Marine "*monthly*" catalogue (index_monthly.txt), the last product update was done in May 2022. Moreover, since the monthly catalogue only includes the last 5 years, in situ data for the year 2017 are currently not available (e.g. after November 2022 (last access for this deliverable), the catalogue data of year 2017 were not further updated). In the downloaded 2017 glider dataset, chlorophyll is the most available BGC variable with 2775 vertical profiles. Few profiles of oxygen are also present for a limited area (i.e., North of Crete) during winter. Given their very limited availability and still on-going activities for a delayed mode quality control procedure, it has been decided to do not consider oxygen data in the present assimilation experiments. BGC-glider data are in NetCDF file format of EGO-gliders (EGO-glider, 2022), and their elaboration level is L2, i.e., they have been quality controlled and flagged by Coriolis/Ifremer, who is the Production Unit integrating ocean glider data in the Copernicus Marine Service.

The number of BGC-gliders with chlorophyll sensor deployed in 2017 is 14 (Figure 2), and the 42 available campaigns are manly distributed in the West Mediterranean Sea. Most of the glider campaigns are in winter (16) and autumn (11); while summer and spring have 8 campaigns each. The BGC-glider campaigns are partly overlapping BGC-Argo float trajectories (orange dots in Figure 2). It is worth to note that not all the PHY-glider missions also provide chlorophyll data (see Figure 1 in the Deliverable D4.2), and the glider missions in the Lev4 subregion (Figure 2) do not have PHY observations.

[1] ftp://nrt.cmems-du.eu/Core/INSITU_MED_NRT_OBSERVATIONS_013_035/med_multiparameter_nrt/

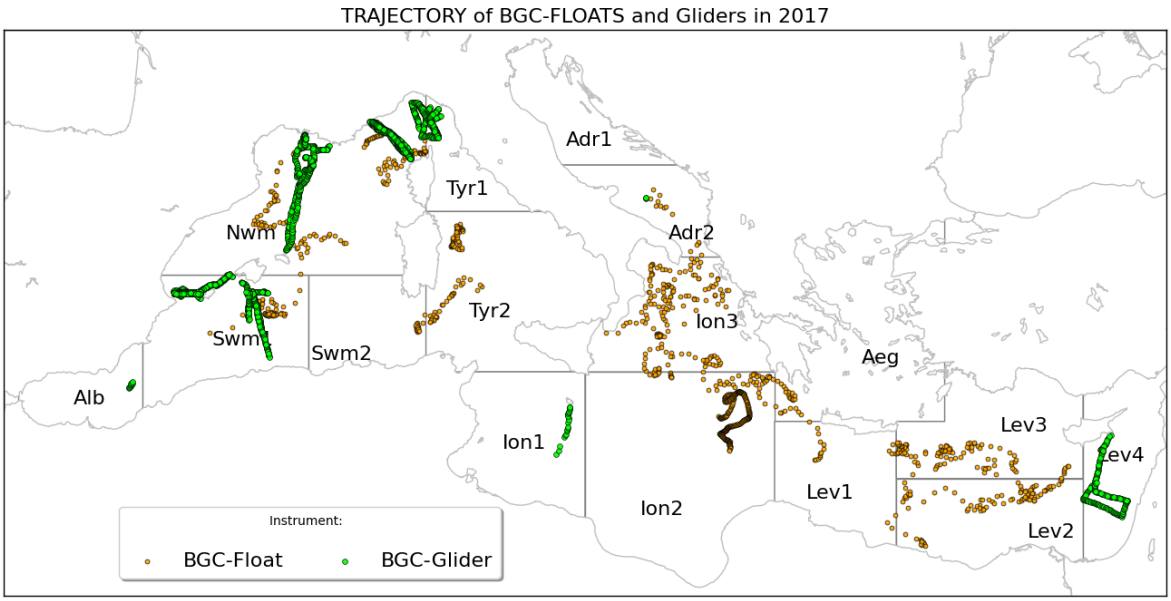

Figure 2. BGC-glider trajectories (green dots) and BGC-Argo profiles (orange dots) for chlorophyll during 2017

3.2. Pre-processing of BGC-glider data

A novel pre-processing procedure has been implemented to prepare BGC-glider chlorophyll observations for the assimilation. The procedure, which is built upon the work by Cotroneo et al. (2019), has been adapted for the specific Mediterranean application and partly described in deliverable D4.2. After the joint WP3-WP4 workshops (24th June 2021) the procedure has been further developed and is briefly summarized in the following sub sections. The procedure is applied independently to each one of the 42 glider campaigns.

Quality Flag and preliminary check on chlorophyll and depth

Only good, probably good, and interpolated data with corresponding quality control (QC) flags 1, 2, and 8 are selected. The obtained dataset is further checked for negative values of chlorophyll and for missing depth data (empty field), which are removed.

Vertical binning and Superobing

For each mission, the quality-controlled profiles are interpolated along a prescribed vertical discretization (i.e. 5 m, with some exceptions where the discretization is set to10 m) to obtain regular sampled vertical profiles. The vertical interpolation is a prerequisite before superobing calculation and application of the vertical and horizontal smoothing filters. Superobing consists of the two spatio-temporal aggregation: (I) the average of the profiles that fall on a given day and in a given grid cell of the Mediterranean model (i.e., resolution of 1/24°) is considered; and (ii) the ascending and descending profiles are averaged.

Interpolation, surface extrapolation and smoothing filter

After superobing, missing values within a profile are filled by using linear interpolation of adjacent values. Following the quality procedure adopted for BGC-Argo floats, if a glider profile lacks values in the upper part (from 0 to a depth not exceeding 35 m), the first available value is extrapolated to the surface. No extrapolation is made for the lower end of the profile. Finally, a vertical and horizontal running mean is

applied as in Cotroneo et al. (2019). Some different sequences of the operations have been tested and compared. The present order of the operation has been chosen after an expert judgment of the resulting transects. Indeed, aggregating profiles before extrapolation decreases the number of blanks inside profiles (Figure 3).

An example of the result of the sequence of the pre-processing is shown in Figure 3 for a glider mission (WMO 61866 in 01-02/2017). The resulting sequence of profiles has no missing values in between and possible sharp discontinuities and anomalous values have been smoothed out.

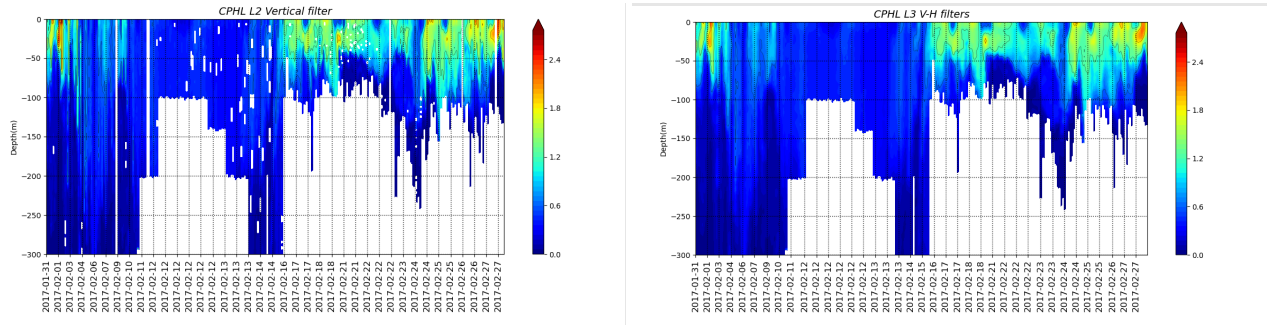

Figure 3. Example of pre-processing BGC-glider chlorophyll: section with raw observations after superobing on Med-MFC grid (left) and after final interpolation and smoothing filter (right)

3.3. Cross-validation of BGC-glider data with ocean colour and BGC-Argo floats

Different technologies are used to retrieve chlorophyll concentration from different sensors: reflectance and empirical algorithms are used for satellite chlorophyll, while florescence and estimated fluorescence-to-chlorophyll ratio are used for the in situ autonomous sensors such as BGC-Argo floats and BGC-gliders. Further, the quality control procedures of the different data streams also differ. As a result, there can be inconsistencies between the different types of measurements of chlorophyll (see for example Figure 4 in D4.2). Therefore, an additional procedure of quality control of BGC-glider chlorophyll data has been implemented through a cross-validation calculation with ocean colour and BGC-Argo float data. The cross-validation of BGC-glider data with ocean colour and BGC-Argo floats is based on the spatial and temporal match up of the measurements and the computation of the Mean Absolute Error (MAE) metric. The computation is made individually for each glider mission and when at least two synchronized measurements are available for at least two different sensors. Results of the cross-validation computation are shown in

Figure 4, where different colours indicate the level of the inconsistency for surface values (upper panel) and for the whole column values (lower panel). Consistent measurements for different sensors are considered for MAE values lower than 0.05mg/m3 (green), intermediate inconsistencies are for MAE in the range of 0.05 and 0.015 mg/m3 (orange), while MAE values greater than 0.15 mg/m3 identify large inconsistency (red).

Considering the cases of synoptic measurements of different sensors, only 30% (25%) of the glider missions can be cross validated at surface (for the whole water column) with the other sensors. Intermediate and large inconsistencies at surface occur during winter (DJFM), while during late summer and autumn a better level of consistency between glider and other instruments (floats and satellites) is observed. The MAE investigation performed below the surface (bottom panel of Figure 4) shows a similar pattern than at surface.

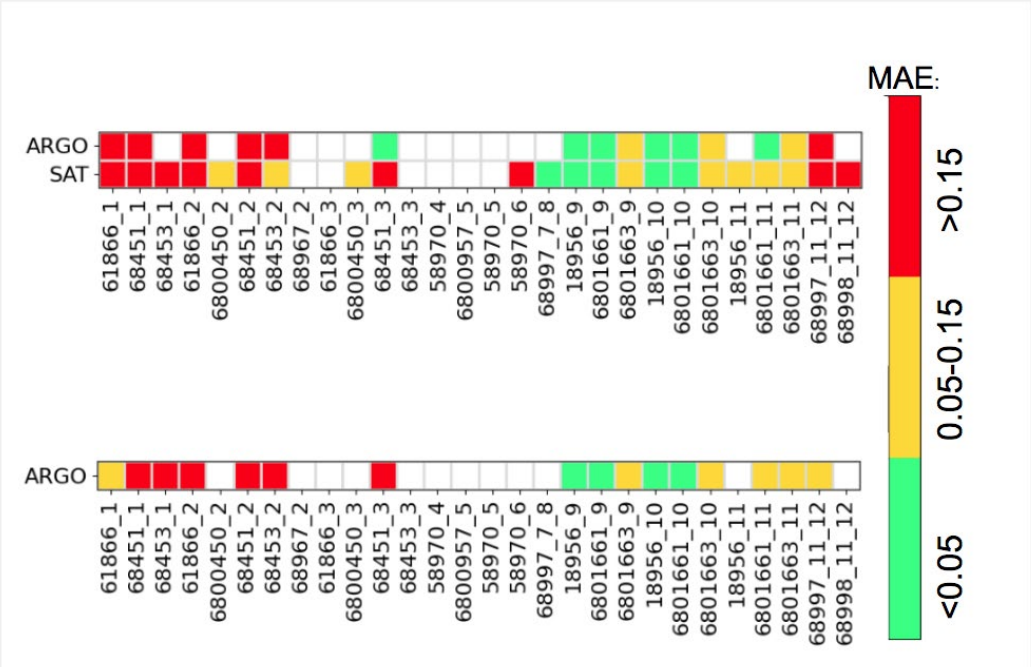

Figure 4. comparison of chlorophyll at surface between glider and satellite and BGC-Argo float (upper panel) and blow the surface between glider and BGC-Argo float profiles (lower panel). Colours indicate small inconsistency in green (MAE lower than 0.05mg/m3), intermediate inconsistency in orange (MAE in the range of 0.05 and 0.015 mg/m3) and large inconsistency in red (MAE greater than 0.15 mg/m3). White colour indicates glider missions that do not have matching with satellite or BGC-Argo float observations.

4. Setup for BGC simulations and BGC-Glider data assimilation

The biogeochemical simulations cover the year 2017 in accordance with the physical glider data assimilation experiments described in Deliverable D4.9.

4.1. Biogeochemical simulation setup

The setup of the MedBFM model system is detailed in Salon et al. (2019) and includes boundary in the Atlantic Ocean and at the Dardanelles Strait, atmospheric forcing for [O2 and CO2] air-sea gas exchanges and nutrients deposition, land forcing for nutrients and carbon input from rivers and ocean dynamics. Differently from the standard setup described in Salon et al., 2019, the initial conditions are derived from a 2-year spin up simulation.

Additionally, the physical ocean (current, temperature, salinity, vertical eddy diffusivity, SSH) are provided by the MedFS system. As described in the next section, two sets of daily physical ocean forcing are used: with and without assimilation of physical-glider data.

Three simulations are performed to assess the impact of physical-glider assimilation on biogeochemistry (ALL_MED_BIO_01) and the benefit of assimilating BGC-glider observations (ALL_MED_BIO_01_BGC). The run ALL_MED_BIO_00 is the reference biogeochemical simulation without biogeochemical assimilation and forced by the output of the ALL_MED_CTL_00 physical simulation. An additional simulation tests the full multiplatform data assimilation (i.e., joint assimilation of ocean colour, BGC-Argo float and BGC-glider) to

demonstrate its feasibility in the contest of the actual configuration of the Mediterranean biogeochemical Analysis&Forecast model system in the Marine Copernicus Service.

Table 1 list of biogeochemical and physical simulations and assimilated observations. Font colours are used in chapter 6 to facilitate the simulation identification.

Name of BGC run	Name of PHY run	Assimilation of PHY-glider observation	Assimilation of BGC-glider observations	Assimilation of BGC-Argo floats and Ocean Colour
ALL_MED_BIO_00	ALL_MED_CTL_00	No	No	No
ALL_MED_BIO_01	ALL_MED_GLD_01	Yes	no	No
ALL_MED_BIO_01_BGC	ALL_MED_GLD_01	Yes	Yes	No
ALL_MED_BIO_01_BGC_multi	ALL_MED_GLD_01	Yes	Yes	Yes

4.2. Physical forcing from MedFS configuration and PHY-glider assimilation

The Copernicus Marine MED-MFC physical component (MedFS) is a coupled hydrodynamic-wave modelling system with data assimilation scheme implemented over the whole Mediterranean Sea extended into the Atlantic Ocean, to which it is connected through the Strait of Gibraltar that provides a net water flux, from 17.29°W to 36.29°E and from 30.19°N to 45.98°N and described in Coppini et al. (2023) and Clementi et al. (2022). The horizontal and vertical resolution are aligned within the MED-MFC as 1/24° and 141 unevenly distributed levels, respectively. The data assimilation system is based on a 3D variational ocean data assimilation scheme, OceanVar, developed by Dobricic and Pinardi (2008) and later upgraded by Storto et al. (2016). The assimilated observations are: along-track sea level anomaly (a satellite product including dynamical atmospheric correction and ocean tides is chosen) from CMEMS SL-TAC, and in- situ vertical temperature and salinity profiles from VOS XBTs (Voluntary Observing Ship-eXpandable Bathythermograph) and ARGO floats from CMEMS INSITU-TAC. Additional details of the MedFS model system and setup implementation are provided in the deliverable D4.9. Here we briefly present two experiments that assess the impact of the glider observations in the MedFS when they are assimilated together with the other in-situ and satellite observations that are already integrated into the system. The experiment ALL_MED_CTL_00 in Table 1 corresponds to the MedFS configuration which assimilates ARGO profilers and altimeter derived SLA observations while relaxing towards OA-SST to correct the surface heat fluxes. In ALL_MED_GLD_01, we ingest the glider observations shown in Figure 5 too. Only ascending profiles are chosen and assimilated while no subsampling is performed on individual profiles. This choice is done partially considering that we assign an increased observation error to the gliders in the R matrix but also, we don't see a major increase in the computational cost in the minimization of the cost function.

It is worth to note that the biogeochemical glider campaigns (Figure 2) are not the same of physical glider campaigns (Figure 5). For example, the physical campaigns east of Balearic Islands have not chlorophyll observations, as well as some of the glider campaigns north of Balearic Islands.

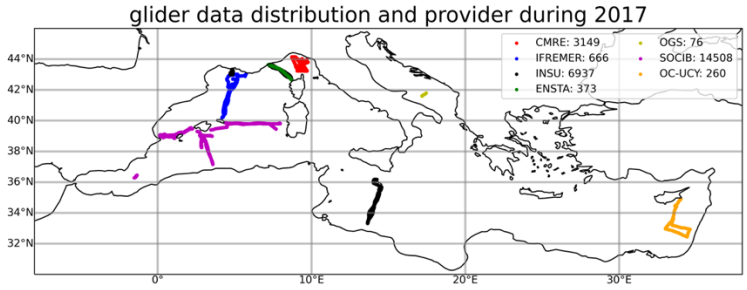

Figure 5. Distribution of the physical glider observations in the entire Mediterranean Sea in 2017. Each colour shows a different provider of observations to Copernicus Marine database.

4.3. Setup for the BGC-glider data assimilation

The assimilation of BGC-glider chlorophyll observations is based on: (i) adoption of a BGC-Argo float-like approach (i.e., the glider missions are considered as sequences of profiles); (ii) latest updates of the 3DVarBio scheme; (ii) daily assimilation cycles and uncorrelated observation error.

In the 3DVarBio scheme, the model error background matrix has the vertical and horizontal covariance components based on synthetic vertical profiles and Gaussian filtering, respectively (see section 2). The synthetic profiles used to describe vertical covariances have been obtained through EOF (empirical orthogonal function) decomposition of the 20-year Mediterranean Sea Copernicus Marine reanalysis. In order to account for the spatial-temporal variability of biogeochemical processes in the Mediterranean Sea, the EOFs have been calculated on a monthly basis over 17 open-ocean and 16 coastal sub-basins. The correlation length scale used in the horizontal Gaussian filter is spatially varying in order to account for the different spatial length scale across the Mediterranean Sea.

In the assimilation scheme the observations are assumed to be uncorrelated, thus the observation covariance matrix is diagonal. The error assigned to BGC-glider chlorophyll observations is monthly varying and tuned through a calibration on prior and posterior misfit between observations and model (Cossarini et al., 2019).

BGC-glider profiles of chlorophyll concentration are assimilated once a day and a single profile is assimilated for each grid cell (see section 3.2 for the pre-processing of the glider observations). Thanks to horizontal covariance the impact of each assimilated profile is spread on areas nearby (the correlation radius is close to 15 km on average).

5. Physical simulations and PHY-glider assimilation

Before presenting the results of the biogeochemical simulations, the present section summarizes the results of the physical simulations highlighting the impact of the PHY-glider assimilation. Details of the results of the physical glider data assimilation are reported in the deliverable D4.9.

The time evolution of the RMSD of temperature and salinity for different depth layers from surface to the deep basin using all in-situ observations is shown in Figure 6. The blue and orange curves show the experiments without and with gliders, respectively. The assimilation of gliders improves in all layers for salinity. RMSD of salinity between 0-10 m reduces from 0.31 to 0.26 which corresponds to a decrease of about 15 %. Between 10-100 and 100-500 m layers it decreases by ~20% and ~7% respectively. In the layer below 500, the salinity RMSD decreases from 0.026 to 0.024 which is approximately an improvement of 8%. For the temperature, except the uppermost layer there is an improvement too. The RMSD of temperature

increases from 0.89 to 0.95 (7%) between 0-10 m layer. There is a significant improvement at the subsurface and deep layers. An improvement of 0.8%, 22% and 14% at the layers between 10-100 m, 100-500 m and 500-1500 m, respectively.

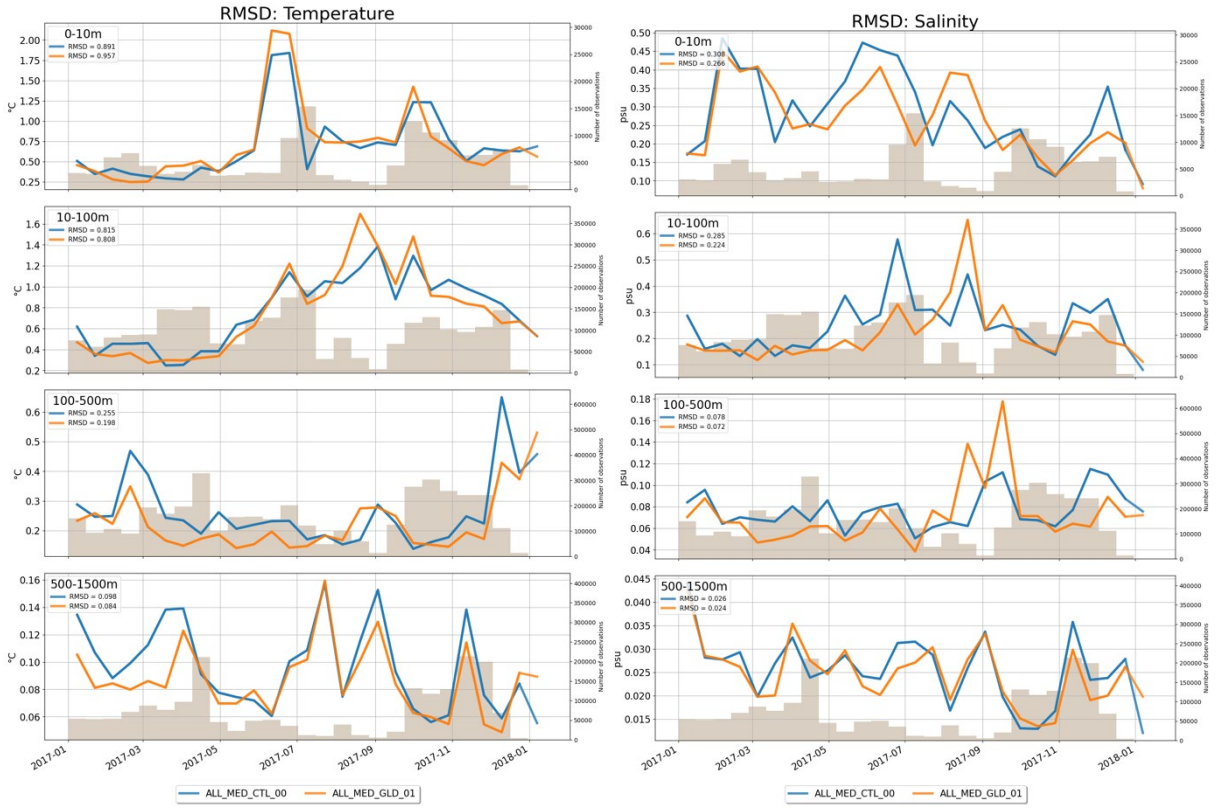

Figure 6. Biweekly timeseries of RMS of temperature (left) and salinity (right) difference for different depth layers (0-10 m, 10-100 m, 100-500 m, 500-1500 m from top to bottom). ALL_MED_CTL_00 (blue) and ALL_MED_GLD_01 (orange). The annual mean RMSD are printed in the legend of each panel. The shaded area shows the number of observations binned every two weeks.

The error evolution of the two experiments can be seen also from the Hovmoller diagrams of temperature and salinity (Figure 7). They confirm the overall improvement of the RMSD with some exceptional time slices. For example, temperature RMSD reduces after September 2017, while between July – September there can be seen some increase in error around the seasonal thermocline depth. As well, in the last week of September there is a degradation especially between 50-100 m depth. These results are consistent with the timeseries in Figure 6. The overall improvement in 2017 is evident from the vertical temperature and salinity profiles of the RMSD and BIAS in Figure 8. RMSD of temperature shows a degradation at the surface layers while salinity is improved everywhere in the water column (left panels). Moreover, Figure 8 shows that bias is reduced in almost all layers for both variables (mid-panels).

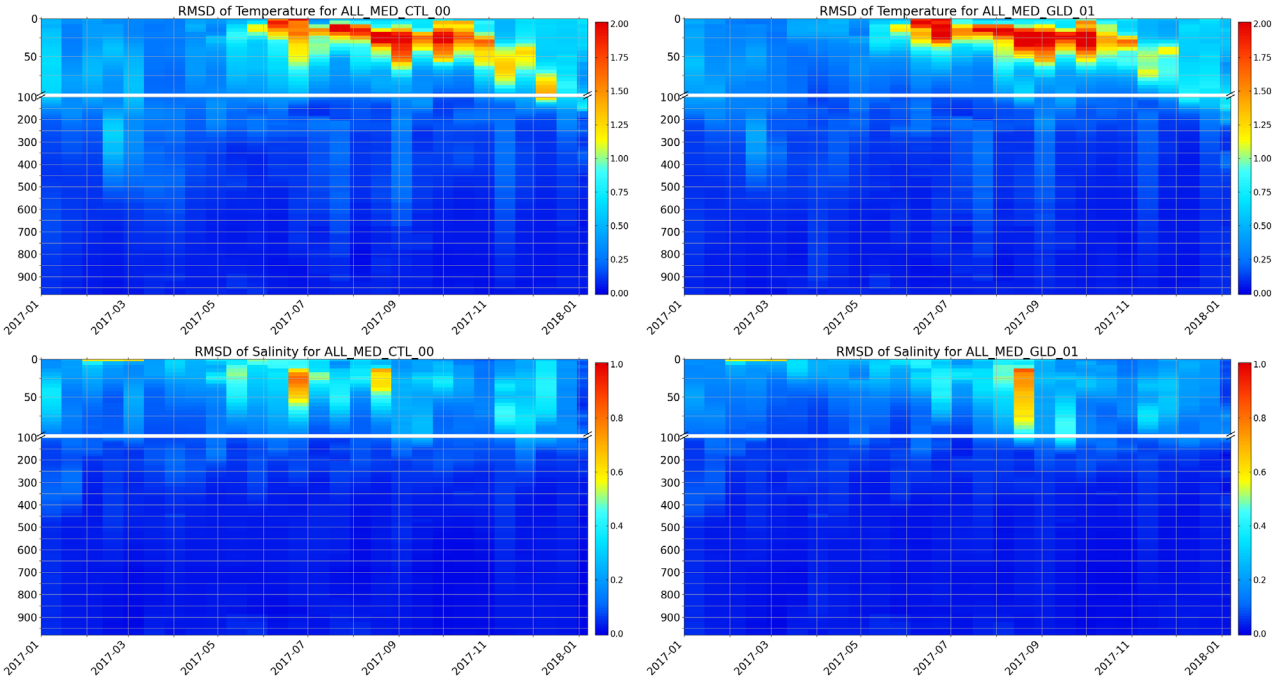

Figure 7. Hovmoller diagrams of RMSD for temperature (upper panels) and salinity (lower panels) for ALL_MED_CTL_00 (left panels) and ALL_MED_GLD_01 (right panels) with a zoom in the first 100 m.

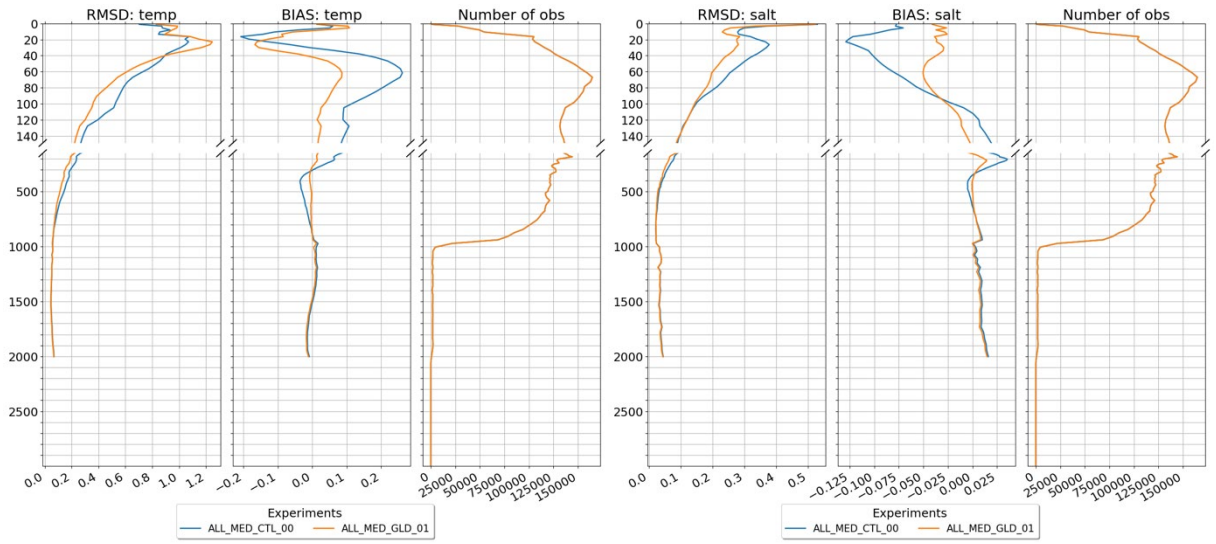

Figure 8. Vertical temperature and salinity profiles of mean RMSD (left) and BIAS (mid) for the ALL_MED_CTL_00 (blue) and ALL_MED_GLD_01 (orange).

6. Results of BGC-Glider data assimilation

The performance of the different simulations (Table 1) are evaluated by comparing the model output with available observations for the assimilated variable (chlorophyll) and for unobserved variables (nitrate and oxygen from BGC-Argo floats). The comparison is done using the model output before the assimilation or the daily average model output for comparison with non-assimilated observations.

The skill performance metrics is the root mean square error (RMSE) and it is computed for opportune spatial subdivision of the Mediterranean model domain (i.e., the 16 subbasins or combination of them; Figure 9) and temporal periods (i.e., winter and summer periods).

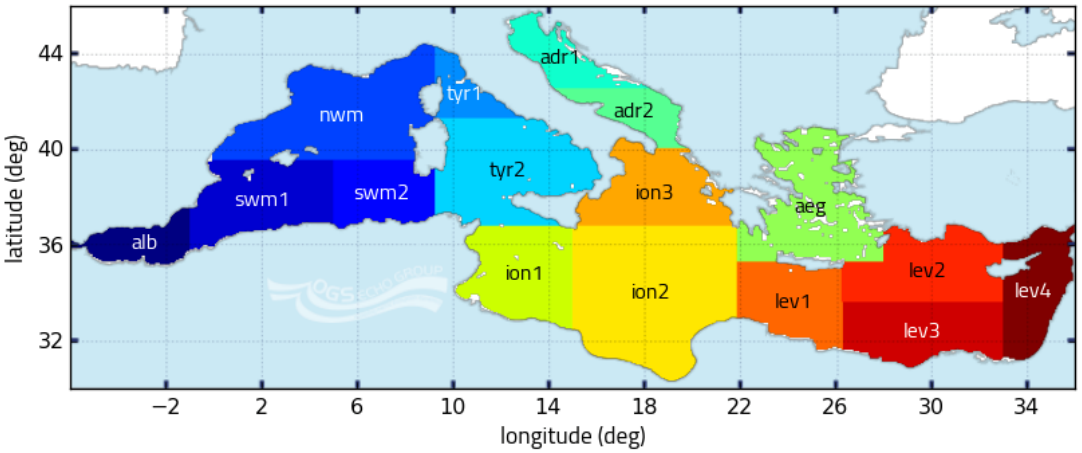

Figure 9. Mediterranean model domain and subdivision in subbasins for the computation of the skill performance metrics. According to data availability and to ensure consistency and robustness of the metrics, different subsets of the sub-basins or some combinations of them can be used for the different metrics: lev=lev1+lev2+lev3+lev4; ion=ion1+ion2+ion3; tyr=tyr1+tyr2; adr=adr1+adr2; swm=swm1+swm2.

6.1. Validation on observed biogeochemical variable (chlorophyll)

The comparison of chlorophyll profile model output with the BGC-glider profiles is done before the assimilation of the observations. Thus, the computed metrics represents a semi-independent validation (i.e., observations can be correlated with the observations of the same sensor assimilated in the previous assimilation cycle). Results of the comparison are shown in Figure 10 for the simulations listed in Table 1. As expected, the assimilation of BGC-glider markedly improves the quality of modelled chlorophyll (orange lines with respect to the black one in Figure 10). The improvements are of 40-60% (i.e., reduction of RMSD with respect to the ALL_MED_BIO_00 run) in all the sub-basins except for Ionian and Levantine ones where the reduction of RMSD is of 5% and 20%, respectively. It must be noted that the errors of the reference run (ALL_MED_BIO_00) are already very low in these two sub-basins. Additionally, the BGC-glider assimilation has always a positive impact even when the PHY-glider assimilation (blue lines in Figure 10) degrades the model output (as for example in the Adr and Ion sub-basins). Finally, the full multiplatform assimilation experiment (ALL_MED_BIO_01_BGC_multi) shows RMSD values that are always higher than the BGC-glider assimilation (ALL_MED_BIO_01_BGC) and even higher than the reference run in two sub-basins (i.e., Adr and Lev). This is a direct result of discrepancies between glider chlorophyll measurements and ocean colour chlorophyll measurements (section 3). Although the full multiplatform experiment assimilates BGC-glider, the greatly higher density of the ocean colour observations and their discrepancy with the BGC-glider

observations cause the model solution to move further away from the BGC-glider observations, which degrades the model metric for this comparison.

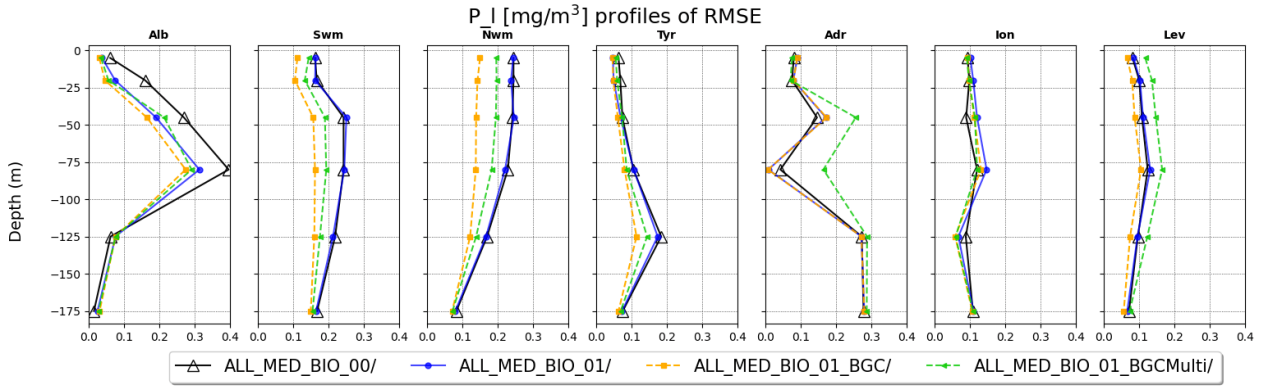

Figure 10. Root Mean Square Error of model chlorophyll versus BGC-glider for the different simulations. The RMSDs are computed over the aggregated subbasins and select vertical layers.

The comparison of surface chlorophyll model output with ocean colour data is shown in Figure 11 for the different simulations. Results show that the glider assimilation, both physical and biogeochemical, has a small impact on the quality of surface chlorophyll. It can be noted that the BGC-glider assimilation very slightly improves the model performance in some cases: aeg, ion3 and lev2 in winter, and nwm, tyr1 and lev2 in summer. On the other hand, the PHY-glider assimilation causes small degradations in swm1, swm2, tyr1 and lev3 in winter, and the addition of the BGC-glider assimilation caused further degradation in swm1 and nwm in winter. The inclusion of the assimilation of ocean colour data improves by 40-60% the RMSE metrics (green bars in Figure 11) as already seen in previous 3DVarBio implementations (Teruzzi et al., 2018; 2021).

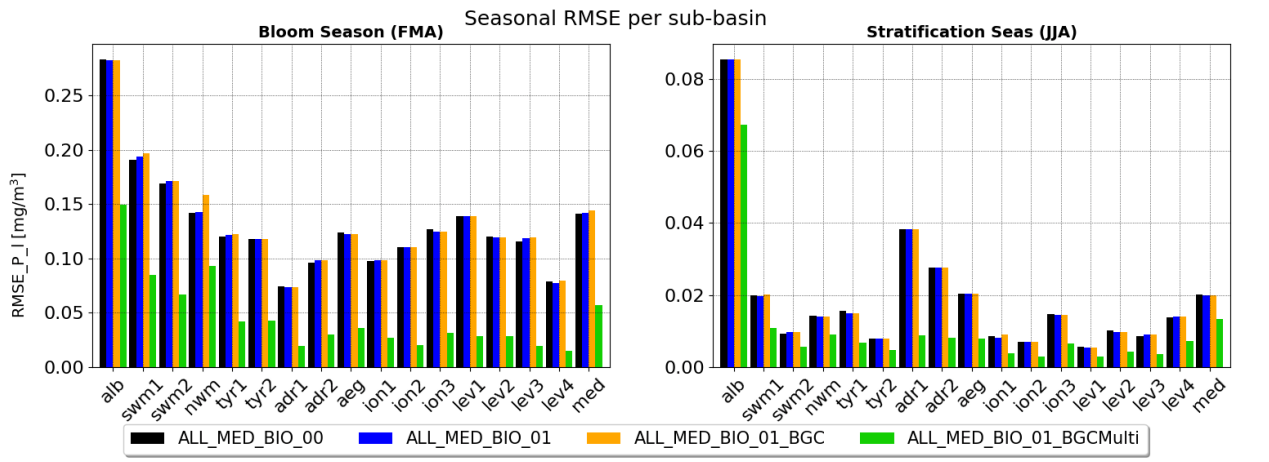

Figure 11. Root Mean Square Error of model surface chlorophyll versus ocean colour for the different simulations. The RMSD is computed over the 16 subbasins and the entire Mediterranean domain (med).

The comparison of modelled chlorophyll profile with profile of BGC-Argo floats (Figure 12) shows that the assimilation of glider data, both physical and biogeochemical observations, has negligible impact for this specific metric. Some factors contributed to downplay this metric: the discrepancies between glider and BGC-

Argo observations showed in section 3.3, the relative limited spatial impact of profiles assimilation and the relatively small number of overlapping glider and BGC-Argo trajectories.

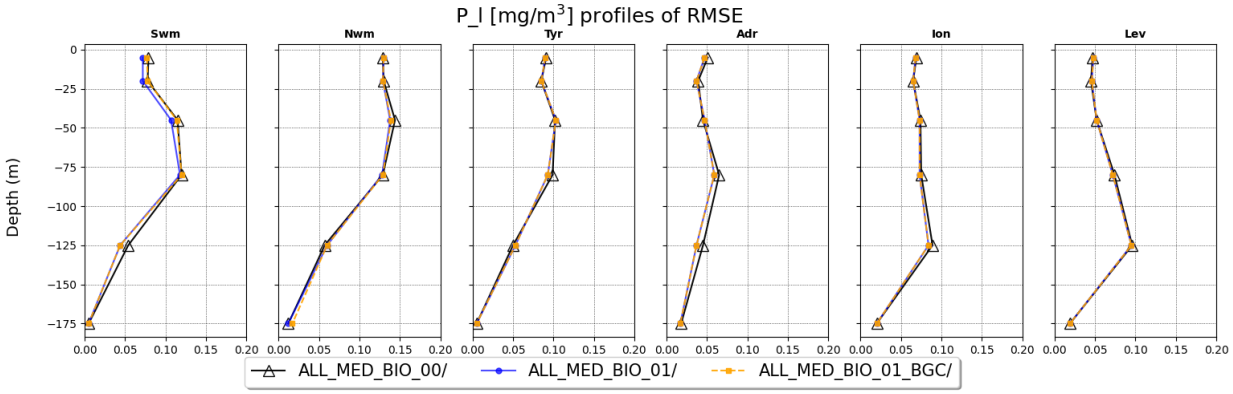

Figure 12. Root Mean Square Error of model chlorophyll versus BGC-Argo floats for the different simulations. The RMSDs are computed over the aggregated subbasins and select vertical layers.

6.2. Validation on non-observed biogeochemical variables

Figure 13 and Figure 14 show the skill performance metrics computed for BGC-Argo nitrate and oxygen, which are two non-observed (i.e., assimilated) variables. Nitrate comparison shows both improvements and degradations of the PHY-glider assimilation and basically no impact of the BGC-glider assimilation. It must be noted that the number of BGC-Argo floats with nitrate sensor is lower than those with chlorophyll sensor (less than 40%), thus resulting statistics might be less reliable. PHY-glider assimilation caused a slightly degradation of oxygen statistics at surface in some subbasins (swm and nwm) due to temperature degradation (section 5, and deliverable D4.9) and its effect on the O2 solubility calculation. In the subsurface layer, a decrease (increase) of the RMSD in swm, nwm and lev (ion) is observed after the PHY-glider assimilation. No impact on the quality of oxygen is observed after the BGC-glider assimilation. The small sensitivity of the oxygen skill performance metrics to the chlorophyll profiles assimilation is already reported by Teruzzi et al. (2021).

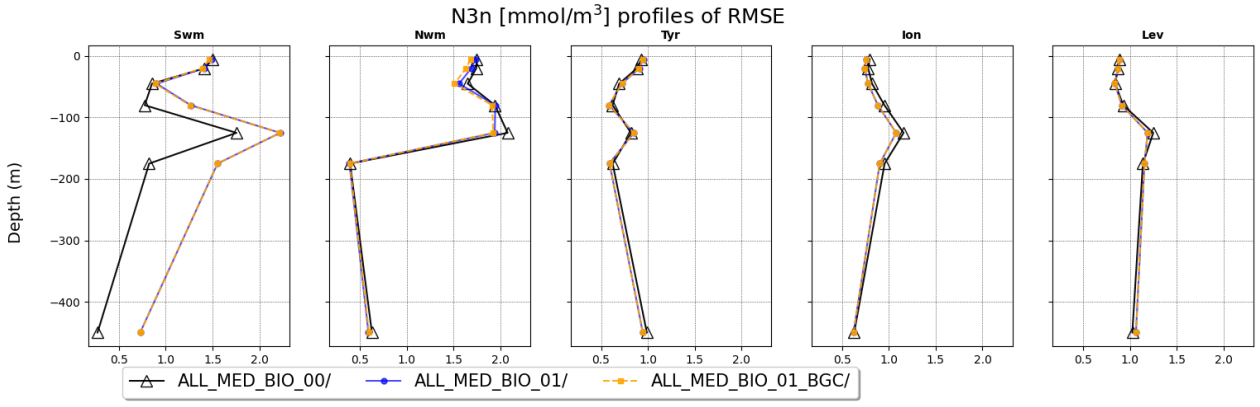

Figure 13 Root Mean Square Error of model nitrate versus BGC-Argo floats for the different simulations. The RMSDs are computed over the aggregated subbasins and select vertical layers.

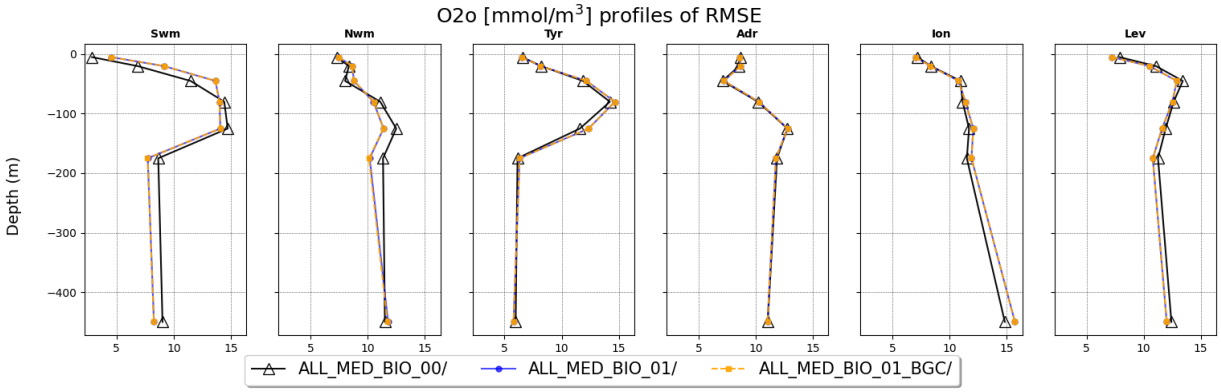

Figure 14. Root Mean Square Error of model oxygen versus BGC-Argo floats for the different simulations. The RMSDs are computed over the aggregated subbasins and select vertical layers.

6.3. Spatial impact of BGC-glider assimilation

Information on the DA area of impact and its temporal persistence are investigated by analysing the changes of assimilated simulations with respect to the reference run (ALL_MED_BIO_00). We use the same impact indicator described in Teruzzi et al. (2021):

$$I_{ij}(t) = \frac{|Sim_{(t)} - Ref_{(t)}|_{300}}{(|Ref|_{300})_{mean}}$$

Where *Ref* is here the reference simulation (ALL_MED_BIO_00) while *Sim* refers to one of the different simulations listed in Table 1. $|Sim(t) - Ref(t)|$ is the absolute difference between simulations (for each day and grid point) while the subscript 300 represents the integral over the 0–300m. The indicator $I_{ij}(t)$ quantifies how much an assimilated run deviates from the *Ref* simulation. Figure 15 (right panel) shows the chlorophyll (left) and nitrate (right) seasonal 95th percentile of the $I_{ij}(t)$ indicator for the three simulations with assimilation with respect to the *Ref*. The 95th percentile of the indicator in ALL_MED_BIO_01 simulation clearly shows that the PHY-glider assimilation impacts both chlorophyll and nitrate. In more than 50% of the Mediterranean Sea surface the 95th percentile of $I_{ij}(t)$ is higher than 0.3, with impacted areas depending on the season. In winter, the largest impacts are localized in the Balearic Channel and in the eastern Levantine, while in summer they are more distributed across the Mediterranean Sea. The addition of the BGC-glider assimilation in simulation ALL_MED_BIO_01_BGC enhances the impact in the Balearic area in winter for chlorophyll but it has limited effects in summer both for chlorophyll and nitrate. Given the fact that corrections by BGC-glider are not very high in the eastern Mediterranean Sea (i.e., the model is already performing well with respect to the BGC-glider; see section 4.1), the index of impact is not much sensitive to the changes during summer. Finally, as already shown in Teruzzi et al. (2021), the inclusion of BGC-Argo and satellite assimilation (ALL_MED_BIO_001_BGCMulti) largely increases the impact factor, especially in winter for chlorophyll and summer for nitrate.

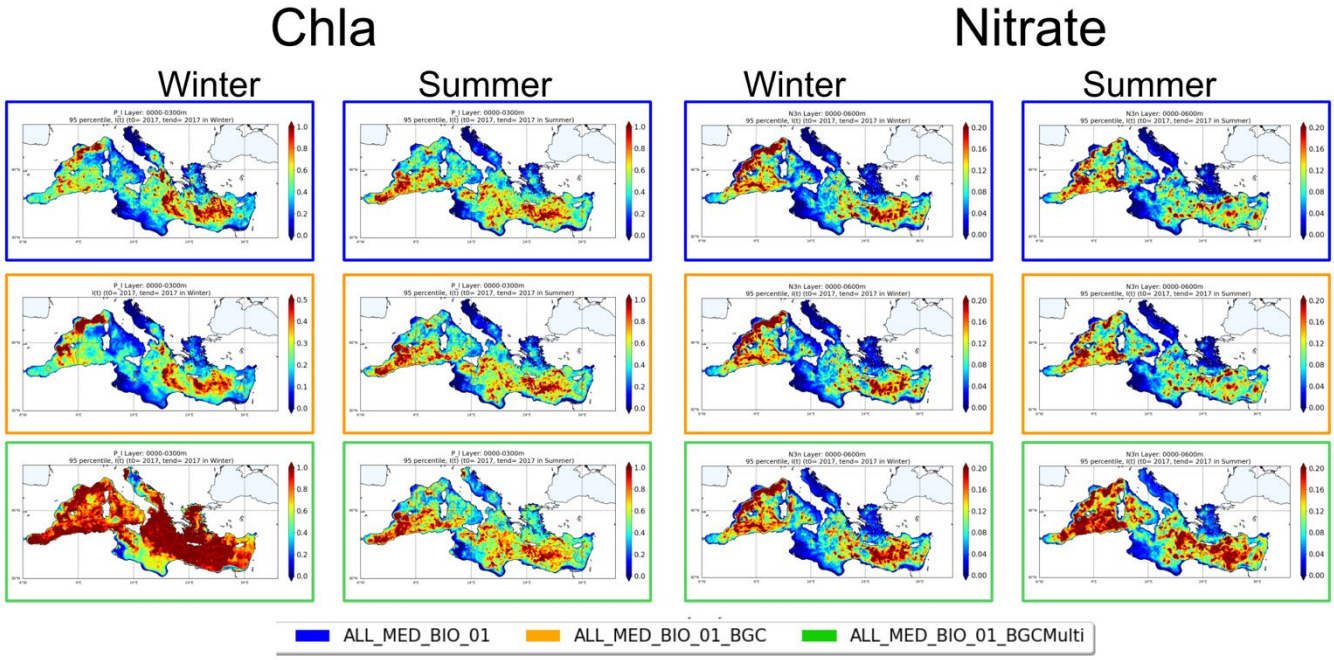

Figure 15. Maps of the $I_{ij}(t)$ 95th percentiles for chlorophyll (first and second columns) and nitrate (third and fourth column) for the three assimilation simulations: only PHY-glider (blue), PHY and BGC-glider (orange) and joint multiplatform assimilation (green). Two seasons (winter and summer) are shown for each variable.

6.4. Impact of PHY and BGC-glider assimilation on ecosystem dynamics

To understand impact of PHY and BGC-glider assimilation on biogeochemical dynamics we investigated primary production, and the vertical dynamics in two specific areas (the Balearic gyre and the areas south of Balearic Islands during autumn 2017).

Primary production

Primary production is the synthesis of organic compounds from dissolved carbon dioxide through photosynthesis as source of energy and, in the BFM model formulation, it considers the contribution of four phytoplankton functional types. Primary production is computed as the vertical integral of the 0-200 m layer and for two selected periods: (i) winter to spot the contribution of the winter phytoplankton blooms and (ii) summer to highlight the contribution of deep chlorophyll maximum (DCM) dynamics to the annual value of primary production of the Mediterranean Sea.

First row of Figure 16 shows the primary production of the reference run, the second row shows the impact of PHY-glider assimilation on primary production with respect to the reference run, while the third and fourth rows report the impact of BGC-glider and of full multiplatform assimilation with respect to ALL_MED_BIO_01 (i.e., the biogeochemical run forced by the physical run with PHY-glider assimilation).

PHY-glider assimilation caused patchy negative and positive variations both in winter and summer (second row of Figure 16), with a very low overall mean seasonal variation: -0.01% and 0.02% in winter and summer, respectively. Physical glider assimilation produces small changes in the mesoscale structures and their effect accumulated during the simulation (e.g., growing in summer w.r.t. winter). These effects in turn propagate through changes in vertical nutrient fluxes and phytoplankton spatial patches, and are eventually spotlighted by the spatial changes in the primary production.

The chlorophyll BGC-glider assimilation has a local impact on primary production clearly visible along the trajectories of the glider missions in three areas: Balearic basin, north-western Mediterranean, and Levantine south of Cyprus. The changes are always positive suggesting that both winter bloom and steady DCM production are underestimated by the model without assimilation. Finally, the full multiplatform biogeochemical assimilation has a clear negative impact on primary production given the overwhelming effect of ocean colour observations, as already seen in Teruzzi et al. (2021). Interesting, the winter map (fourth row of Figure 11) shows that the impact of the BGC-glider assimilation counterbalances the ocean colour effects in specific areas, such as the north-western Mediterranean Sea.

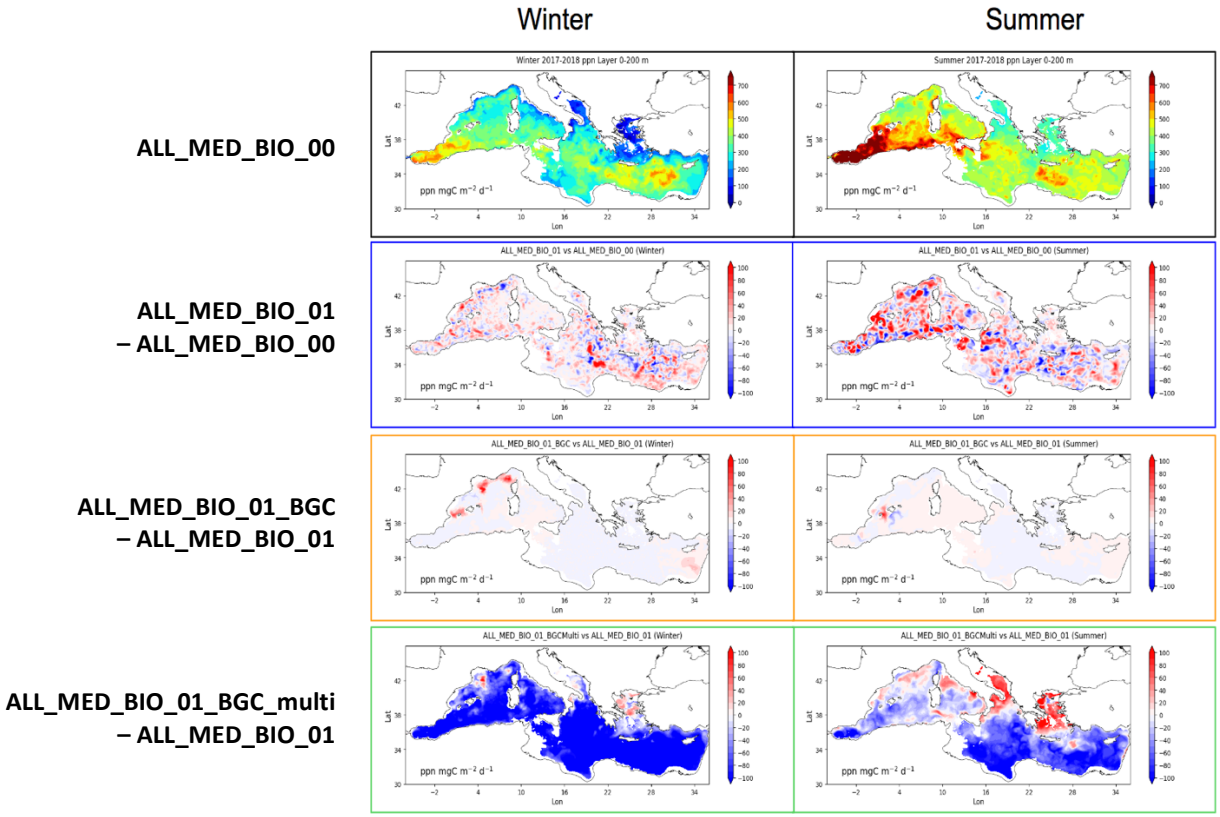

Figure 16. Map of net primary production [NPP, mgC m-2 d-1] for winter and summer periods for the Ref simulation (first row, black box). Maps of NPP difference between ALL_MED_BIO_01 and Ref (second row, blue box), between ALL_MED_BIO_01 and ALL_MED_BIO_00 (third row, orange box) and ALL_MED_BIO_01_BGC_multi and ALL_MED_BIO_01 (forth row, green box).

Vertical dynamics in specific areas

The case study of the Balearic gyre during autumn 2017, which is presented in deliverable D4.9, allows us to investigate the impact of PHY-glider assimilation on biogeochemical vertical dynamics. Figure 17 shows that the addition of the PHY-glider assimilation (ALL_MED_GLD_01) produces a more delimited and round shaped anticyclonic gyre than the physical simulation without glider assimilation (ALL_MED_GLD_00). This is more evident in the December map. The comparison with satellite SSH data (first row in Figure 17) confirms that the model is more consistent with satellite when PHY-glider are assimilated. Despite the bias between modelled chlorophyll and satellite during the autumn bloom, Figure 18 shows that the addition of PHY-glider assimilation improves the correspondence of the gyre pattern (i.e., round hole of low chlorophyll concentration in the centre of the gyre and higher concentration at its border) between ALL_MED_BIO_01 and satellite in December. Indeed, the correlation between satellite and simulations increase from 0.46 (ALL_MED_BIO_00) to 0.58 (ALL_MED_BIO_01). The BGC-glider assimilation produces no impact because

autumn glider missions in that areas do not have chlorophyll observations. Finally, the Figure 19 illustrates that the reason of the positive impact of PHY-glider assimilation is due to a better simulation of the downwelling effect of the anticyclonic cycle in December. Indeed, when the PHY-glider data are assimilated the concentration of chlorophyll in the central part of the anticyclonic gyre is decreased consistently with the surface satellite chlorophyll map.

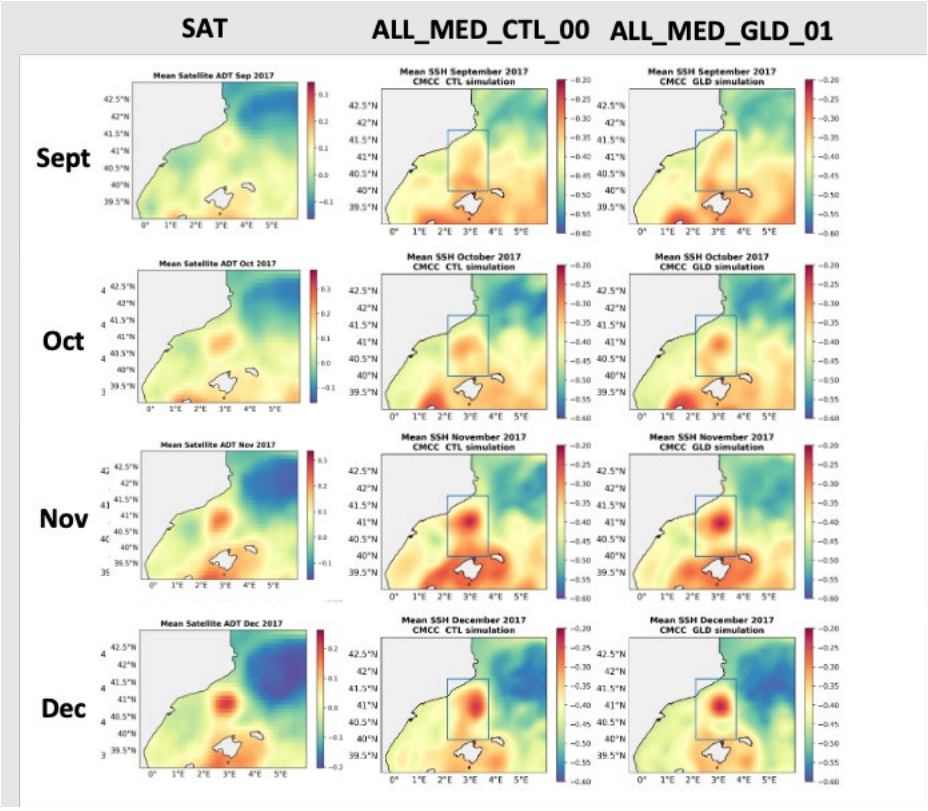

Figure 17. Monthly map of SSH (m) in the north Balearic areas for the satellite (first column) and the two physical simulations: without PHY-glider assimilation (second column) and with PHY-glider assimilation (third column). Figures and results from deliverable D4.9.

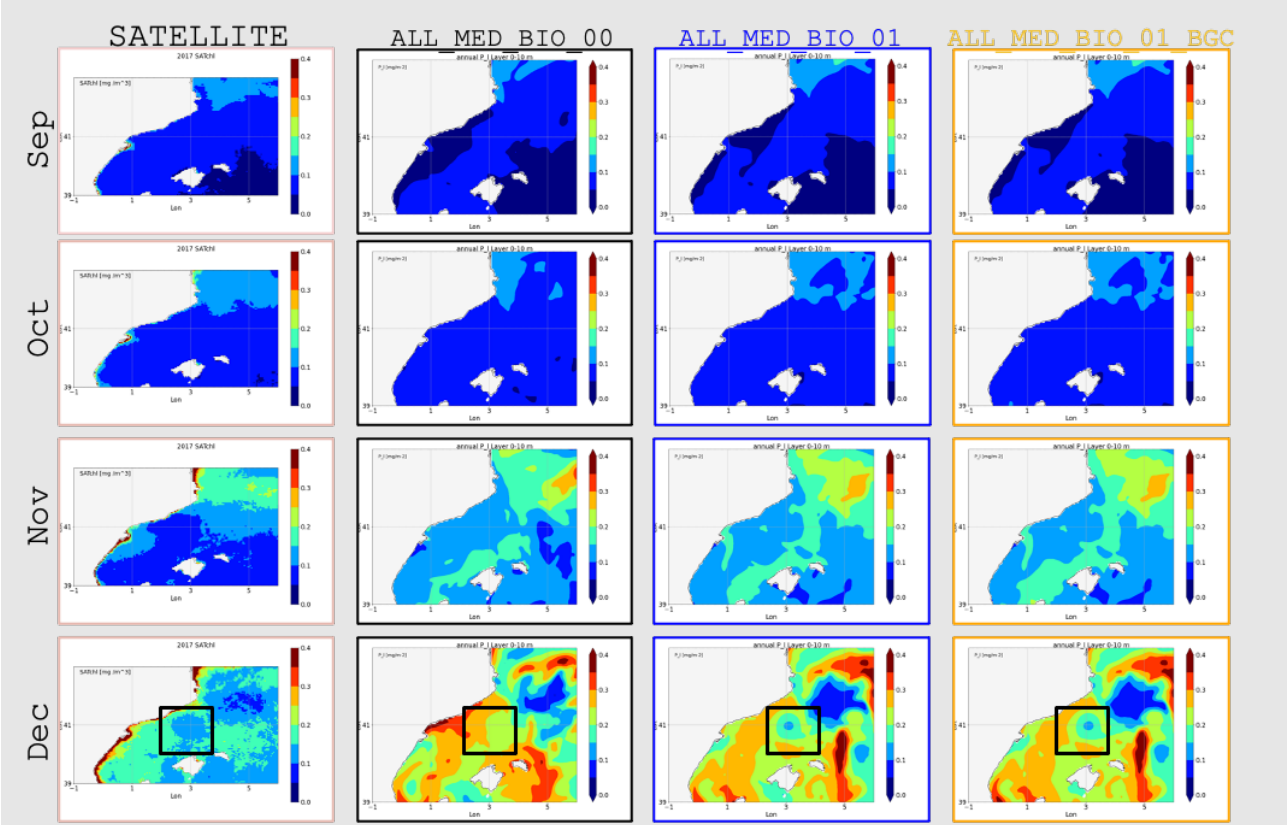

Figure 18. Monthly map of surface chlorophyll (mg/m3) in the north Balearic areas for the satellite (first column) and three biogeochemical simulations: ALL_MED_BIO_00 (second column, black boxes), ALL_MED_BIO_01 (third column, blue boxes) and ALL_MED_BIO_01_BGC (forth column, orange boxes). Inner black boxes in the December maps indicate the area over which the correlation is computed.

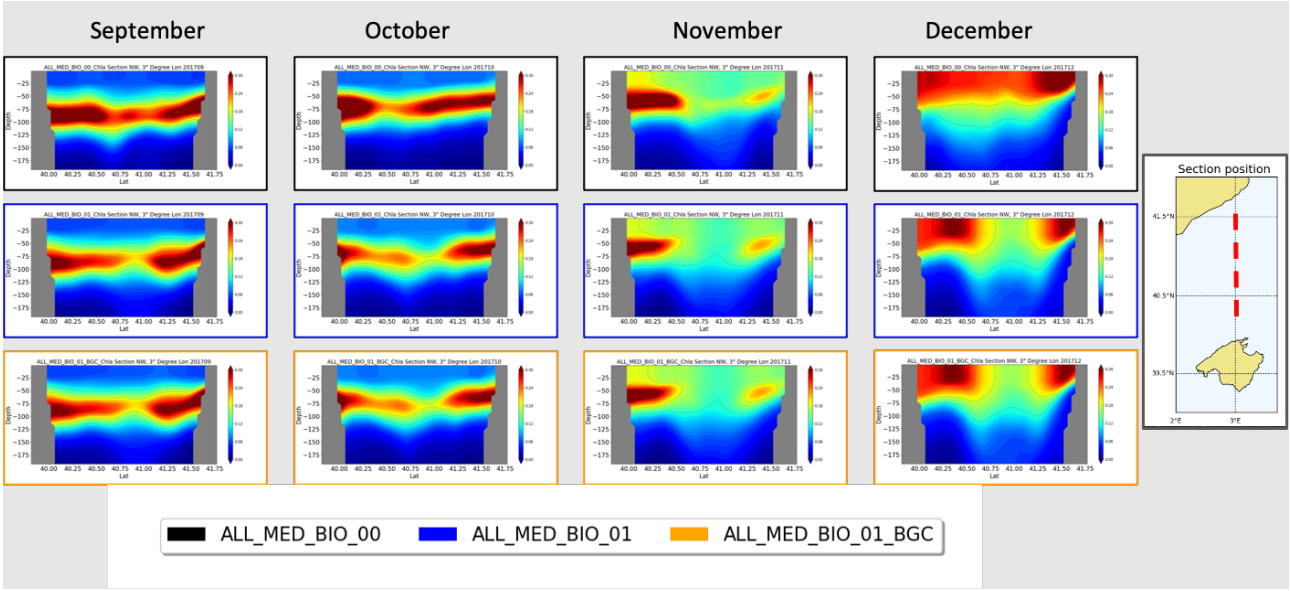

Figure 19. Section of chlorophyll monthly averages at Lon=3° in the northern Balearic basin for the three biogeochemical simulations: ALL_MED_BIO_00 (first row, black boxes), ALL_MED_BIO_01 (second row, blue boxes) and ALL_MED_BIO_01_BGC (third row, orange boxes).

Considering a section south of Balearic Islands (Figure 20) during autumn 2017, the results show the positive effect of the BGC-glider assimilation during the transition phase between summer stratification to autumn condition with vertical mixing and surface bloom. The October section (Figure 20) show well-established DCM dynamics across the whole area. Neither physical nor biogeochemical glider assimilation impacts the model, that already simulates well this end of summer stratification condition. During November, the vertical mixing starts to erode stratification and the DCM structure. Biogeochemical glider assimilation corrects a possible too strong impact of the physical glider assimilation, restoring the intensity of the DCM dynamics and increasing the chlorophyll concentration at surface (second and third rows in the second column in Figure 20). Finally, in December, the BGC-glider assimilation improves the previous two simulations (i.e., both the reference and the PHY-glider assimilation simulations) by increasing the concentration of the surface bloom, its extension toward south and the thickness of the surface layer involved in the bloom in the northern part of the section. Figure 21, which shows the comparison of BGC-Argo, BGC-glider and model profiles in the overlapping area of glider and float profiles (Lon=3.30° and Lat=38.75°, left panel in Figure 21), confirms that the assimilation of glider data allows to better simulate the transition between summer stratification and mixed autumn condition with surface bloom. During November (central panel in Figure 21), the presence of a deep chlorophyll maximum structure is already well simulated by the reference run (black line in Figure 21) and the assimilation runs change only slightly the vertical chlorophyll profiles. BGC-Argo float profiles also confirm the good model performances. Then, during December (right panel in Figure 21), the shape of chlorophyll profile is corrected by the BGC-glider assimilation by increasing the intensity of surface bloom in the areas south of Balearic Islands. Finally, it is worth to note that the multiplatform assimilation (fourth row of Figure 20 and green lines in Figure 21), which includes the Ocean Colour observations, reduces remarkably the impact of the only glider data assimilation during December.

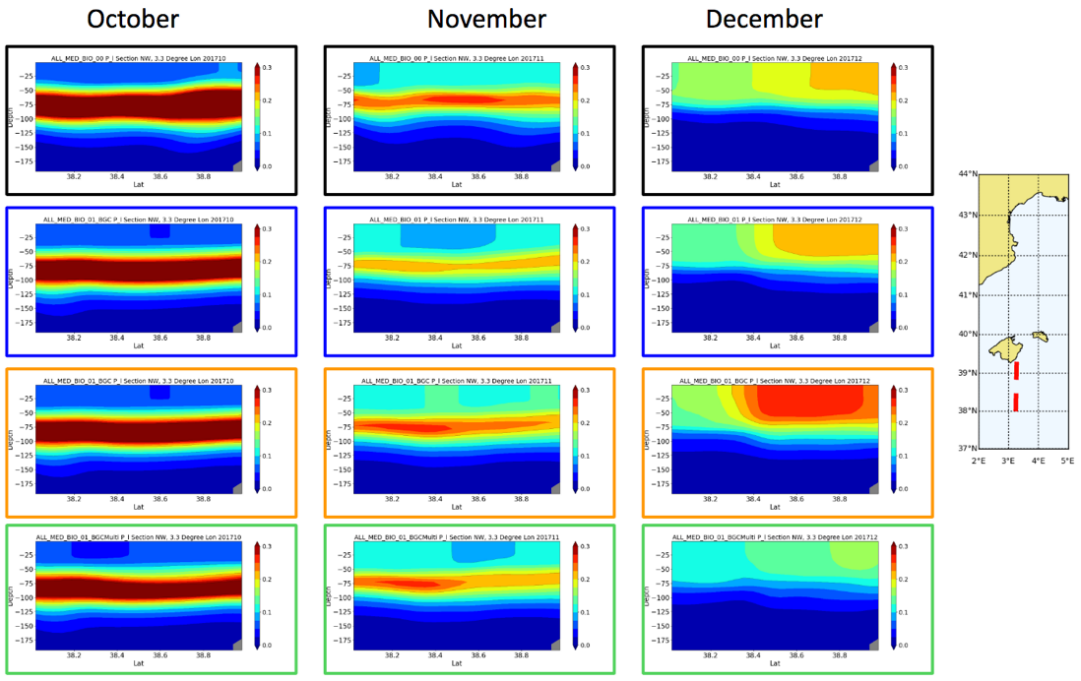

Figure 20. Section of chlorophyll monthly averages at Lon=3.5° in the area south of the Balearic Islands for the three biogeochemical simulations: ALL_MED_BIO_00 (first row, black boxes), ALL_MED_BIO_01 (second row, blue boxes), ALL_MED_BIO_01_BGC (third row, orange boxes) and ALL_MED_BIO_01_BGC_multi (fourth row, green boxes)

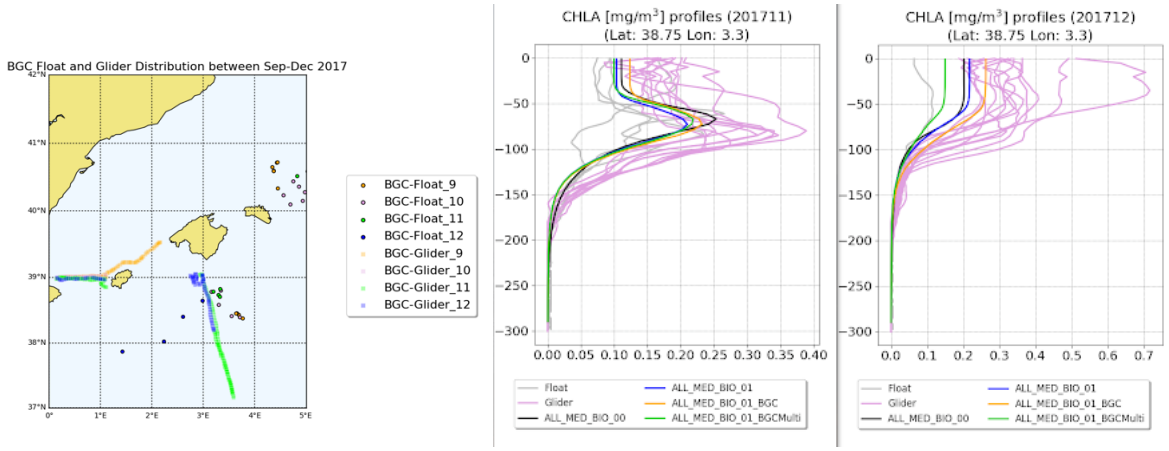

Figure 21. Positions of profiles of glider and BGC-Argo during September-December 2017 (left panel). Chlorophyll profiles of BGC-glider, BGC-Argo float and the different simulations for November and December 2017 (central and right panels).

Conclusion

The present deliverable aims at showing the importance and benefit of the assimilation of vertical profiles in biogeochemical models. This represents a relevant improvement with respect to the biogeochemical operational models (such as those used in the Marine Copernicus Service) where the assimilation mainly relies on satellite ocean colour observations. Specifically, for the Mediterranean Sea Copernicus model, the present deliverable shows the novelty of the assimilation of profiles from BGC-glider which is complementary to the BGC-Argo float assimilation shown in Teruzzi et al (2021). Finally, the deliverable reports an analysis of the impact of the assimilation of physical variables observed by glider on biogeochemical dynamics.

Results of the simulations show that the assimilation of biogeochemical profiles is beneficial for improving biogeochemical modelled vertical dynamics (i.e., DCM, nitracline, flux of nutrients) and is complementary to surface observation assimilation. As shown in Cossarini et al. (2019) and in Teruzzi et al. (2021) for BGC-Argo and satellite joint assimilation, satellite chlorophyll observations are relevant in winter when the upper part of the water column is well mixed and the biological dynamics develops mostly at surface, while chlorophyll profiles are important in summer when the biological dynamics develop in the subsurface layer (i.e., at the DCM depth above the nutricline) and surface and subsurface are more uncoupled because of stratification. Unfortunately, the limited availability of glider campaigns during summer prevented a clear and robust confirmation of this conclusion.

BGC-glider represents an important source of BGC profiles, often complementary to BGC-Argo (e.g., different areas covered and different strategy of sampling). However, at the present stage BGC-glider data (retrieved from standard repository such as Copernicus Marine in situ TAC) need pre-processing to filter high frequency noise and discontinuity in profiles. Additionally, the tested BGC-glider repository (Copernicus Marine in situ TAC) seems in a continuous process of improving the storage and visibility of the data that, however, does not facilitate the use of the data in an operational and real time framework.

Further, the inconsistencies of chlorophyll concentration from different sensors (i.e., reflectance from ocean colour and fluorescence from in situ sensors) represent a potential risk when multisource of biogeochemical data are used without precaution. In any case, our results show that the multiplatform data assimilation and model dynamical adjustment can act as a filter for inconsistencies of the observations from multiple sources.

Considering all validation datasets, the simulation that assimilates all observation sources (ALL_MED_BIO_01_BGC_multi) performs better than any single data stream assimilation. In fact, the model simulation remains in between the data distributions of the different sensors.

The variational assimilation scheme uses a horizontal spatial error covariance operator based on correlation radius length scales that are of the order of the mesoscale dynamics. Thus, the impact of the BGC-glider (chlorophyll) data assimilation is relevant basically only along the glider mission. It is important to identify glider mission trajectories along relevant areas to target specific processes. On the other hand, the PHY-glider assimilation or the assimilation of profiles of other biogeochemical variables (as done for BGC-Argo data) can have a wider spatial impact given their cascading and memory effects on ecosystem dynamics (Teruzzi et al, 2021).

Finally, the assimilation of PHY-glider demonstrates a positive effect itself on biogeochemical variables with further improvements when also BGC-glider chlorophyll is assimilated. Indeed, the BGC-glider assimilation after PHY-glider assimilation can increase the consistency between physical and biogeochemical processes in the model simulation. Generally, the update of both physical and biogeochemical field through an assimilation scheme that preserves consistency between the two is a preferable option than assimilating only physical information (Bertino et al., 2022)

References

Bertino, L. and SEALESS team, 2022. D4.2 Recommendations for strongly coupled physical-biogeochemical data assimilation. Deliverable report of project H2020 SEAMLESS (grant 101004032.). doi 10.5281/zenodo.7432230

Bethoux, J. P., Morin, P., Chaumery, C., Connan, O., Gentili, B., and Ruiz-Pino, D., 1998. Nutrients in the Mediterranean Sea, mass balance and statistical analysis of concentrations with respect to environmental change, Mar. Chem., 63, 155–169.

Bittig, H. C., Maurer, T. L., Plant, J. N., Schmechtig, C., Wong, A. P., Claustre, H., Xing, X., 2019. A BGC-Argo guide: Planning, deployment, data handling and usage. Frontiers in Marine Science, 6, 502.

Canu, D. M., Ghermandi, A., Nunes, P. A., Lazzari, P., Cossarini, G., Solidoro, C., 2015. Estimating the value of carbon sequestration ecosystem services in the Mediterranean Sea: An ecological economics approach. Global Environmental Change, 32, 87-95.

Ciavatta, S., Kay, S., Saux-Picart, S., Butenschön, M., & Allen, J. I., 2016. Decadal reanalysis of biogeochemical indicators and fluxes in the North West European shelf-sea ecosystem. Journal of Geophysical Research: Oceans, 121(3), 1824-1845.

Clementi, E., Pistoia, J., Escudier, R., Delrosso, D., Drudi, M., Grandi, A., Lecci, R., Cretí, S., Ciliberti, S., Coppini, G., Masina, S., Pinardi, N., 2022. Mediterranean Sea Analysis and Forecast (CMEMS MED-Currents EAS5 system, 2019-2021) [Data set]. Copernicus Monitoring Environment Marine Service (CMEMS), https://doi.org/10.25423/CMCC/MEDSEA_ANALYSIS_FORECAST_PHY_006_013_EAS6.

Coppini, G., Clementi, E., Cossarini, G., Salon, S., Korres, G., Ravdas, M., Lecci, R., Pistoia, J., Goglio, A. C., Drudi, M., Grandi, A., Aydogdu, A., Escudier, R., Cipollone, A., Lyubartsev, V., Mariani, A., Cretì, S., Palermo, F., Scuro, M., Masina, S., Pinardi, N., Navarra, A., Delrosso, D., Teruzzi, A., Di Biagio, V., Bolzon, G., Feudale, L., Coidessa, G., Amadio, C., Brosich, A., Miró, A., Alvarez, E., Lazzari, P., Solidoro, C., Oikonomou, C., and Zacharioudaki, A., 2023. The Mediterranean forecasting system. Part I: evolution and performance, EGUsphere [preprint], https://doi.org/10.5194/egusphere-2022-1337.

Cossarini, G., Lazzari, P., Solidoro, C., 2015. Spatiotemporal variability of alkalinity in the Mediterranean Sea. Biogeosciences, 12(6), 1647-1658.

Cossarini, G., Mariotti, L., Feudale, L., Mignot, A., Salon, S., Taillandier, V., d'Ortenzio, F., 2019. Towards operational 3D-Var assimilation of chlorophyll Biogeochemical-Argo float data into a biogeochemical model of the Mediterranean Sea. Ocean Modelling, 133, 112-128.

Cossarini, G., Feudale, L., Teruzzi, A., Bolzon, G., Coidessa, G., Solidoro, C., Salon, S., 2021. High-resolution reanalysis of the Mediterranean Sea biogeochemistry (1999–2019). Frontiers in Marine Science, 8, 1537.

Cotroneo, Y., Aulicino, G., Ruiz, S., Sánchez Román, A., Torner Tomàs, M., Pascual, A., Budillon, G., 2019. Glider data collected during the Algerian basin circulation unmanned survey. Earth System Science Data, 11(1), 147-161.

Dobricic, S., Pinardi, N., 2008. An oceanographic three-dimensional variational data assimilation scheme. Ocean Modelling, 22, 3-4, 89-105.

EGO-gliderm, 2022. EGO Gliders Data Management Team (202-) EGO gliders NetCDF format reference manual NetCDF conventions Reference tables and files distribution Version 1.3. IFREMER, 67pp. DOI: 10.13155/34980

Fennel, K., Gehlen, M., Brasseur, P., Brown, C. W., Ciavatta, S., Cossarini, G., and GODAE OceanView Marine Ecosystem Analysis and Prediction Task Team., 2019. Advancing marine biogeochemical and ecosystem reanalyses and forecasts as tools for monitoring and managing ecosystem health. Frontiers in Marine Science, 6, 89.

Fontana, C., Brasseur, P., & Brankart, J. M., 2013. Toward a multivariate reanalysis of the North Atlantic Ocean biogeochemistry during 1998–2006 based on the assimilation of SeaWiFS chlorophyll data. Ocean Science, 9(1), 37-56.

Ford, D., & Barciela, R., 2017. Global marine biogeochemical reanalyses assimilating two different sets of merged ocean colour products. Remote Sensing of Environment, 203, 40-54.

Foujols, M.-A., Lévy, M., Aumont, O., Madec, G., 2000. OPA 8.1 Tracer Model Reference Manual. Institut Pierre Simon Laplace, pp. 39.

Gehlen, M., Barciela, R., Bertino, L., Brasseur, P., Butenschön, M., Chai, F., Simon, E., 2015. Building the capacity for forecasting marine biogeochemistry and ecosystems: recent advances and future developments. Journal of Operational Oceanography, 8(sup1), s168-s187.

Hu, J., Fennel, K., Mattern, J. P., & Wilkin, J., 2012. Data assimilation with a local Ensemble Kalman Filter applied to a three-dimensional biological model of the Middle Atlantic Bight. Journal of Marine Systems, 94, 145-156.

Kaufman, D. E., Friedrichs, M. A., Hemmings, J. C., & Smith Jr, W. O., 2018. Assimilating bio-optical glider data during a phytoplankton bloom in the southern Ross Sea. Biogeosciences, 15(1), 73-90.

Krom, M.D., Kress, N., Brenner, S., Gordon, L.I., 1991. Phosphorus limitation of primary productivity in the eastern Mediterranean Sea. Limnology and Oceanography, 36(3) 424-432.

Lazzari, P., Teruzzi, A., Salon, S., Campagna, S., Calonaci, C., Colella, S.,Tonani, M. & Crise, A. (2010). Pre-operational short-term forecasts for Mediterranean Sea biogeochemistry. Ocean Science, 6(1), 25-39

Lazzari, P., Solidoro, C., Ibello, V., Salon, S., Teruzzi, A., Béranger, K., Colella, S., and Crise, A., 2012. Seasonal and inter-annual variability of plankton chlorophyll and primary production in the Mediterranean Sea: a modelling approach. Biogeosciences, 9, 217-233.

Lazzari, P., Solidoro, C., Salon, S., Bolzon, G., 2016. Spatial variability of phosphate and nitrate in the Mediterranean Sea: a modelling approach. Deep Sea Research I, 108, 39-52.

Lazzari, P., Álvarez, E., Terzić, E., Cossarini, G., Chernov, I., D'Ortenzio, F., & Organelli, E., 2021. CDOM spatiotemporal variability in the Mediterranean Sea: a modelling study. Journal of Marine Science and Engineering, 9(2), 176.

Lueker, T. J., Dickson, A. G., and Keeling, C. D., 2000. Ocean pCO2 calculated from dissolved inorganic carbon, alkalinity, and equations for K1 and K2: validation based on laboratory measurements of CO2 in gas and seawater at equilibrium, Mar. Chem., 70, 105–119.

Mattern, J. P., Edwards, C. A., & Moore, A. M., 2018. Improving variational data assimilation through background and observation error adjustments. Monthly Weather Review, 146(2), 485-501.

Mehrbach, C., Culberson, C. H., Hawley, J. E., and Pytkowitcz, R. M., 1973. Measurements of the apparent dissociation constants of carbonic acid in seawater at atmospheric pressure, Limnol. Oceanogr., 18, 897–907.

Nerger, L., & Gregg, W. W., 2007. Assimilation of SeaWiFS data into a global ocean-biogeochemical model using a local SEIK filter. Journal of Marine Systems, 68(1-2), 237-254.

Nerger, L., & Gregg, W. W. (2008). Improving assimilation of SeaWiFS data by the application of bias correction with a local SEIK filter. Journal of marine systems, 73(1-2), 87-102.

Orr, J. C., & Epitalon, J. M. (2015). Improved routines to model the ocean carbonate system: mocsy 2.0. Geoscientific Model Development, 8(3), 485-499.

Pradhan, H. K., Voelker, C., Losa, S. N., Bracher, A., & Nerger, L., 2019. Assimilation of global total chlorophyll OC-CCI data and its impact on individual phytoplankton fields. Journal of Geophysical Research: Oceans, 124(1), 470-490.

Salon, S., Cossarini, G., Bolzon, G., Feudale, L., Lazzari, P., Teruzzi, A., Solidoro, C., Crise, A., 2019. Novel metrics based on Biogeochemical Argo data to improve the model uncertainty evaluation of the CMEMS Mediterranean marine ecosystem forecasts. Ocean Science, 15(4), 997-1022.

Simon, E., Samuelsen, A., Bertino, L., & Mouysset, S., 2015. Experiences in multiyear combined state–parameter estimation with an ecosystem model of the North Atlantic and Arctic Oceans using the Ensemble Kalman Filter. Journal of Marine Systems, 152, 1-17.

Storto, A., Masina, S., & Navarra, A., 2016. Evaluation of the CMCC eddy-permitting global ocean physical reanalysis system (C-GLORS, 1982–2012) and its assimilation components. Quarterly Journal of the Royal Meteorological Society, 142(695), 738-758.

Teruzzi, A., Dobricic, S., Solidoro, C., Cossarini, G. 2014. A 3D variational assimilation scheme in coupled transport biogeochemical models: Forecast of Mediterranean biogeochemical properties, Journal of Geophysical Research, doi:10.1002/2013JC009277.

Teruzzi, A., Bolzon, G., Salon, S., Lazzari, P., Solidoro, C., Cossarini, G., 2018. Assimilation of coastal and open sea biogeochemical data to improve phytoplankton simulation in the Mediterranean Sea. Ocean Modelling, 132, 46-60

Teruzzi, A., Di Cerbo, P., Cossarini, G., Pascolo, E., Salon, S., 2019. Parallel implementation of a data assimilation scheme for operational oceanography: the case of the MedBFM model system. Computers & Geosciences 124, 103-114.

Teruzzi, A., Bolzon, G., Feudale, L., & Cossarini, G., 2021. Deep chlorophyll maximum and nutricline in the Mediterranean Sea: emerging properties from a multi-platform assimilated biogeochemical model experiment. Biogeosciences, 18(23), 6147-6166.

Testor, P., De Young, B., Rudnick, D. L., Glenn, S., Hayes, D., Lee, C. M., Wilson, D., 2019. OceanGliders: a component of the integrated GOOS. Frontiers in Marine Science, 6, 422.

Tsiaras, K. P., Hoteit, I., Kalaroni, S., Petihakis, G., & Triantafyllou, G., 2017. A hybrid ensemble-OI Kalman filter for efficient data assimilation into a 3-D biogeochemical model of the Mediterranean. Ocean Dynamics, 67, 673-690.

Verdy, A., & Mazloff, M. R., 2017. A data assimilating model for estimating Southern Ocean biogeochemistry. Journal of Geophysical Research: Oceans, 122(9), 6968-6988.

Wanninkhof, R. (2014). Relationship between wind speed and gas exchange over the ocean revisited. Limnology and Oceanography: Methods, 12(6), 351-362.